ELASTIC AND PLASTIC STABILITY OF ORTHOTROPIC CYLINDERS

By George Gerard

Allied Research Associates

SUMMARY

By utilizing linear stability theory, solutions for elastic buckling of short and moderate length orthotropic cylinders under axial compression are presented and correlated with experimental results on circumferentially stiffened cylinders. The plastic buckling of short and moderate length isotropic and orthotropic cylinders is also investigated and the theoretical results correlated with available experimental data. A discussion of the effects of finite deflections and initial imperfections is presented in order to explain the correlation obtained between the theory and the experimental data.

INTRODUCTION

It is the objective here to summarize the significant results obtained on an NASA sponsored investigation* into the general instability characteristics of stiffened circular cylinders[1-4]. One of the major results of this program was the development of a linear general stability theory for elastic and plastic buckling of orthotropic cylindrical shells under axial compression, external pressure and torsion over the complete length range and the correlation obtained with experimental data.

Since linear theory was employed, it is particularly important for shells to correlate the theory with experimental results. Consequently, all available data on stiffened and unstiffened shells were correlated with the theory on a unified basis. For the lateral pressure case, the experimental results were in good agreement with the predictions of the linear theory[1]. Under torsional loading, the stiffened cylinder data exhibited somewhat more scatter but were in reasonably good agreement with the linear theory to the same extent

*NASA Research Grant NSG-17-59 with New York University

that the unstiffened cylinder data correlated[1]. Thus, it was concluded that for lateral pressure and torsion, linear theory provides a satisfactory approach.

For orthotropically stiffened cylinders under axial compression, which is the area of greatest interest in launch and space vehicle applications, there was almost a complete lack of published test data. As a consequence, an experimental program was conducted on machined orthotropic cylinders of 2014-T6 aluminum alloy under axial compression. In all cases the stiffening system consisted of circumferential rings.

The test data obtained in this program[4] when compared to the predictions of the linear stability theory revealed a most significant trend. Most of the test data fell within 90 to 100 percent of the linear theory which is in remarkable contrast with the corresponding isotropic cylinder case where the test data generally fall at a small fraction of the linear theory. Furthermore, the test data on the circumferentially stiffened cylinders which were obtained primarily on 8 in. diameter cylinders exhibited relatively little scatter. Corresponding tests on several larger diameter cylinders indicated no significant scale effect.

The theoretical reasons advanced for the behavior of the circumferentially stiffened cylinders are related to the fact that such cylinders first buckle in the axisymmetric mode[3]. Since this mode is stable in the post-buckling region, the deleterious effects of initial imperfections are minimized and circumferentially stiffened shells fail close to the predictions of linear theory.

SYMBOLS

A_1 plasticity coefficient, $A_1 = (1/4)(1 + 3\ E_t/E_s)$

B_i extensional rigidity, $B_i = E_s t_i/(1 - \nu^2)$

$\bar{B}/B_3$ $4(A_1 - \nu^2)(B_2/B_3) - \nu(B_1 + B_2)/B_1$

D_i flexural rigidity, $D_i = E_s I_i/(1-\nu^2)$

$\bar{D}/D_1$ $[\nu(D_1 + D_2) + D_3]/D_1$

E modulus of elasticity

E_s	secant modulus
E_t	tangent modulus
I_i	moment of inertia per unit width
k_x	compressive buckling coefficient
k_{asy}	buckling coefficient, asymmetric mode
k_{axi}	buckling coefficient, axisymmetric mode
L	length
m	number of longitudinal half wave lengths
n	number of circumferential wave lengths
N	loading per unit width
R	radius
t_i	extensional thickness
U	buckling coefficient ratio, $U = k_{asy}/k_{axi}$
w	radial displacement
x,y	coordinates
Z	cylinder curvature parameter, $Z^2 = B_2L^4/12R^2D_1$
Z_o	lower limit of short cylinder region
Z^*	upper limit of short cylinder region
α	$\alpha = B_1D_2/B_2D_1$
β	wavelength parameter, $\beta = nL/m\pi R$
$\bar{\beta}$	see Eq.(1)
β^*	wavelength parameter for moderate length region
γ	$\gamma = B_3\bar{D}/\bar{B}D_1$

δ $\quad \delta = 4\, A_1 B_2 B_3^2 / B_1 \bar{B}^2$

η $\quad$ plasticity reduction factor

$\bar{\eta}$ $\quad$ see Eq.(9)

ν $\quad$ Poisson's ratio

ν_e $\quad$ elastic value of Poisson's ratio

σ $\quad$ axial stress

ELASTIC STABILITY OF ORTHOTROPIC CYLINDERS

The basic solutions for the compressive stability of orthotropic cylinders for the axisymmetric and asymmetric modes, and the behavior of these solutions over the length ranges associated with flat plates, short cylinders and moderate length cylinders was presented in Ref. 3. We shall be concerned here with a review of the essential results.

Moderate Length Range

In the moderate length range, the wavelength parameters for the asymmetric mode m and β can be treated as continuous variables. As a consequence, the following result is obtained for the wavelength ratio,

$$\bar{\beta}^2 = \beta^2 \left(2 \frac{B_2}{B_1} \frac{B_3}{\bar{B}}\right) = \frac{\delta}{2}\left\{\frac{1-\alpha}{\alpha-\gamma} \pm \left[\left(\frac{1-\alpha}{\alpha-\gamma}\right)^2 + \frac{4}{\delta}\frac{1-\gamma}{\alpha-\gamma}\right]^{1/2}\right\} \qquad (1)$$

where:

$$\alpha = B_1 D_2 / B_2 D_1$$

$$\gamma = B_3 \bar{D} / \bar{B} D_1$$

$$\delta = 4\, A_1 B_2 B_3^2 / B_1 \bar{B}^2$$

By use of Eq.(1), the following solution for asymmetric buckling of moderate length orthotropic cylinders can be obtained

$$k_x = 0.702(A_1 - \nu^2)^{1/2} ZU \tag{2}$$

where:
$$U = \left[\frac{\alpha\bar{\beta}^2 + \gamma}{\bar{\beta}^2 + 1}\right]^{1/2} \tag{3}$$

Aside from the factor U, Eq.(2) is identical with that for the axisymmetric mode.

From the definitions of k_x and Z and the solutions for k_x given by Eq.(2) the buckling load for a moderate length cylinder is

$$N_{cr} = \frac{0.702\pi^2}{(12)^{1/2}} \frac{(B_2D_1)^{1/2}}{R} (A_1 - \nu^2)^{1/2} U \tag{4}$$

It is apparent that in cases where $U < 1$ the asymmetric mode will govern while for $U > 1$ the axisymmetric mode will govern.

Since for the asymmetric mode U depends upon $\bar{\beta}$ which, in turn, depends upon the three orthotropic parameters, α, β and δ, it is of interest to examine Eq.(1) in some detail. It is immediately apparent that real or imaginary values of $\bar{\beta}$ can be obtained for various combinations of α and γ. In fact, the critical combinations are $\alpha = \gamma$ and $\gamma = 1$ as illustrated in Fig. 1.

Here, the shaded areas enclosed by the lines $\gamma = \alpha$ and $\gamma = 1$ represent the regions where β is imaginary for asymmetric buckling. Since the axisymmetric mode is real in the entire domain, it is reasonable to assume that buckling in the axisymmetric mode is the only one possible in the shaded regions.

A further study of Eqs.(1) and (3) for the regions where β is real reveals that $U < 1$ for $\gamma < 1$ and that $U > 1$ for $\gamma > 1$. Consequently, the asymmetric mode is theoretically possible in the region $\gamma \leq 1$ for $\alpha \geq \gamma$ only. On the other hand, the axisymmetric mode governs in the remainder of this domain by virtue of either $U > 1$ or imaginary β for the asymmetric mode.

Of further interest is the location of the solution for the isotropic cylinder which lies at the point 1,1. In terms of β this is rather a confused region since theoretically $-\infty < \beta < \infty$. In fact, direct solution of the isotropic elastic cylinder case from the eighth-order Donnell equation results in an indeterminacy for β. However, by proceeding to the limit of the isotropic cylinder from the orthotropic cylinder solution, it is found that for $\alpha = 1$, Eq.(1) reduces directly

to

$$\beta = (A_1 B_1 / B_2)^{1/4} \tag{5}$$

Since Eq.(5) is valid along $\alpha = 1$ as shown in Fig. 1, and this includes the isotropic cylinder point, the indeterminacy in β is removed. In fact, for the isotropic elastic cylinder, Eq.(5) reduces to $\beta = 1$.

A study of the orthotropic parameters indicates that longitudinally stiffened moderate length cylinders are defined by $\alpha < 1$. Similarly, circumferentially stiffened cylinders are defined by $\alpha > 1$. Furthermore, for many practical types of stiffened construction, it appears that γ is not greatly different from unity. Thus, it appears that the region γ, $\alpha < 1$ contains all practical longitudinally stiffened cylinders. The region $\alpha > \gamma > 1$ appears to contain all practical circumferentially stiffened cylinders that buckle in the axisymmetric mode. For the former, both α and γ are important in determining U and hence the buckling load, whereas for the circumferentially stiffened case $U = 1$ theoretically for α, $\gamma > 1$.

Short Cylinder Range

Now that the moderate length range has been considered in some detail, we turn to the short cylinder range where the wavelength parameter $m = 1$, the lowest integer value. For the axisymmetric case, the results shown in Fig. 2 for the $\beta = 0$ case are obtained for all orthotropic elastic cylinders ($A_1 = 1$). At

$$Z = \pi^2/[12(1-\nu^2)]^{1/2} \tag{6}$$

the short cylinder solution merges with the 45° dashed line which represents the moderate length solution given by Eq.(2). However, to be strictly correct, it is necessary to take into account the integer values of m in this region. Consequently, the cusps shown for $m = 2$, 3, 4... are obtained.

For the asymmetric case, β is constant in the moderate length range and is given by Eq.(1). We now denote this value of the wavelength parameter by β^*. It can be observed from Fig. 2 that the lowest value of Z corresponding to this value of β^* is denoted by Z^* which marks the upper limit of the short cylinder region for the particular orthotropic cylinder depicted.

For the asymmetric mode, $0 < \beta \leq \beta^*$ in the short cylinder range and m = 1. The lowest value of Z for the asymmetric mode denoted by Z_o is given by

$$Z_o = \frac{\pi^2 A_1 \gamma^{1/2}}{[12(A_1 - \nu^2)]^{1/2}} \tag{7}$$

The corresponding value of k_x for Z_o is

$$k_x = A_1(1 + \gamma) \quad ; \quad \text{for } Z = Z_o \tag{8}$$

This value of k_x is the lowest value at which the asymmetric mode can occur. Thus, the short cylinder region for this mode is bounded by $Z_o < Z \leq Z^*$.

In the short cylinder region of Fig. 2, the axisymmetric mode governs below $Z_o = 1.4$ as obtained from Eq.(7) for $\gamma = 1/4$. In the region between Z_o and $Z^* = 27.4$, a numerical procedure given in Ref. 3 was used to obtain the asymmetric curve shown in Fig. 2. At Z^*, the short cylinder curve merges with the dashed line representing the moderate length solution given by Eq.(2) where $\beta^* = 1.074$ in this case and U = 0.619. As in the axisymmetric case, the cusps in the moderate length region result from using the integer values m = 1, 2, 3... and $\beta^* = 1.074$.

PLASTIC STABILITY OF CYLINDERS

In the previous section the solution for elastic buckling of a moderate length isotropic cylinder was obtained as the limiting case of an orthotropic cylinder. Because of the additional complexities that are introduced when plastic buckling is considered, it appears desirable to treat the plastic stability of an isotropic cylinder in some detail before considering the orthotropic cylinder.

In Ref. 2, explicit solutions for plastic buckling of an isotropic cylinder in the axisymmetric and asymmetric modes were obtained for the flat plate and moderate length regions. It is the objective here to present plastic buckling solutions for the short cylinder region and also to define the ranges of validity of the two explicit

solutions for the isotropic cylinder.

For the moderate length region of the plastic isotropic cylinder in terms of the parameters of Fig. 1, $\alpha = 1$ and $\gamma = (2A_1-1)^{-1}$. Thus, the effect of plasticity is to move vertically upward from the isotropic elastic point (1,1) as shown in Fig. 1 as E_t/E_s decreases. As a consequence, the axisymmetric solution should always govern for moderate length cylinders subject to plastic buckling.

Short Cylinder Range

By utilizing the procedures given in Ref. 3, k_x-Z curves have been computed for values of $E_t/E_s = 0.75, 0.50, 0.25$ and 0. The data for the axisymmetric mode are shown in Fig. 3. It can be observed that the axisymmetric plastic solutions closely resemble the elastic case and that for the limiting case $E_t/E_s = 0$, the solution is independent of Z and corresponds to the flat plate solution.

It is convenient to separate out the plasticity effects through the use of a plasticity reduction factor defined as

$$\bar{\eta} = \eta \frac{(1-\nu^2)E}{(1-\nu_e^2)E_s} = \frac{(k_x)_{plastic}}{(k_x)_{elastic}} \tag{9}$$

By use of the plasticity reduction factor, the elastic and plastic buckling load can be jointly written as

$$N_x = \frac{\pi^2 \eta k_x E I_1}{(1-\nu_e^2)L^2} \tag{10}$$

Following Eq.(9), values of $\bar{\eta}$ have been determined for the axisymmetric and asymmetric modes. These data are presented in Fig. 4 and cover the Z-range from flat plates through the short cylinder region into the moderate length region.

In the flat plate region $\bar{\eta}$ corresponds to the explicit solution

$$\bar{\eta} = (1/4)(1 + 3\, E_t/E_s) \tag{11}$$

In the moderate length region, the following explicit solutions of Ref. 2 apply. For the axisymmetric case,

$$\bar{\eta} = (E_t/E_s)^{1/2} \tag{12}$$

For the asymmetric case,

$$\bar{\eta} = \left(\frac{E_t}{E_s}\right)^{1/2} \left[\frac{2 + (1+3\ E_t/E_s)^{1/2}}{3(E_t/E_s) - 1 + (1 + 3\ E_t/E_s)^{1/2}}\right]^{1/2} \tag{13}$$

Orthotropic Cylinders

Although the asymmetric load may be lower than the axisymmetric load for certain cases of elastic buckling of orthotropic cylinders as shown in Fig. 2, it is to be expected from the plastic isotropic cylinder investigation that this situation will reverse itself as E_t/E_s is reduced sufficiently. Since the asymmetric buckling load as well as this crossover point are functions of the orthotropic parameters as well as E_t/E_s, it is evident that it is hardly feasible to construct k_x - Z charts covering a significant range of parameters.

The axisymmetric solution is independent of the orthotropic parameters and therefore the form of the plastic buckling solution for orthotropic cylinders is identical with that for isotropic cylinders as shown in Ref. 2. As a consequence, the data presented in Figs. 3 and 4 for the axisymmetric mode may be used directly for short and moderate length orthotropic cylinders.

For the asymmetric plastic case, the procedure used to construct Fig. 2 for the elastic orthotropic cylinder may be used directly by inserting the proper value of A_1 in the pertinent equations. To illustrate the influence of plasticity upon a moderate length orthotropic cylinder, consider the point $\alpha = 1/2$, $\gamma = 1/4$ which corresponds to the orthotropic cylinder example used in Fig. 2. Although α does not depend upon A_1, γ does, and therefore as A_1 decreases in the plastic range, the effect upon Fig. 1 is to move vertically upward from the point 1/2, 1/4. Beyond the 1/2, 1/2 point, it is apparent that the axisymmetric solution will govern.

CORRELATION WITH EXPERIMENTAL DATA

For moderate length cylinders under axial compression, it is of

particular importance to correlate theoretical results with experimental data because of the well known discrepancy that exists for isotropic elastic cylinders. Consequently, the test data obtained in Ref. 4 for elastic buckling of circumferentially stiffened orthotropic cylinders are presented. In addition, available test data on isotropic plastic cylinders are also presented in order to check another phase of the general theory.

Orthotropic Elastic Cylinders

In Ref. 4, experiments were conducted primarily on a series of 8 in. diameter circumferentially stiffened elastic cylinders of moderate length under axial compressive loading. In terms of the parameters of Fig. 1, the range of stiffening parameters covered $3 < \alpha < 20$ (closely spaced to widely spaced rings) and in all cases $\gamma > 1$. The cylinders were designed such that local instability did not occur before failure in the general instability mode. Because of the fact that $\gamma > 1$ for all cylinders, theoretically they should all buckle initially in the axisymmetric mode.

The test data on the failing strength of each cylinder is shown in Fig. 5 as compared to the results of the linear axisymmetric orthotropic theory. It can be observed that excellent agreement exists in remarkable contrast with the results obtained for isotropic elastic cylinders. The small experimental scatter evident in Fig. 5 together with the good correlation with linear theory are important indications of the potential reliability of this type of construction.

Isotropic Plastic Cylinders

Available test data on the failure strength of moderate length aluminum alloy cylinders that buckled plastically have been assembled in Fig. 6. The test data include low[5], medium[6] and high[7] strength aluminum alloys and thus cover a broad range of interest. The cylinders that could be identified as failing in the axisymmetric and asymmetric modes are so indicated in Fig. 6. Also included for comparison is the axisymmetric plasticity reduction factor for moderate length cylinders as given by Eq.(12). In each case, the theoretical curves were computed by using the compressive stress strain data associated with the test specimens.

It can be observed from Fig. 6, in distinct contrast with well known results for the elastic case, that the axisymmetric buckling theory is in relatively good agreement with the test data for the aluminum alloy cylinders that failed in the axisymmetric mode. On the other hand, the 7075-T6 cylinders that failed in the asymmetric mode in the region between the proportional limit and compressive yield

strength exhibit the discrepancy with linear theory characteristic of the elastic case.

POST-BUCKLING BEHAVIOR OF CYLINDERS

From the correlation between theory and test data obtained in the previous section, it is apparent that the orthotropic and plastic aspects of the problem can have a profound influence on the post-buckling behavior. Consequently, we shall be concerned now with a qualitative evaluation of this region. Because of the obvious complexities of the finite deflection, non-linear features of this region, much of this discussion is somewhat conjectural. It is indeed fortunate, however, that the non-linear features of elastic orthotropic cylinders have been investigated by Thielemann[8] and that Lee[5] has similarly treated the plastic isotropic cylinder.

Elastic Cylinders

A schematic representation of the behavior of perfect, elastic, moderate length cylinders is illustrated in Fig. 7 in terms of the axisymmetric buckling parameters. It can be observed for the isotropic cylinder that the axisymmetric and asymmetric buckling loads are equal and that the post-buckling behavior for the asymmetric mode is unstable whereas that for the axisymmetric mode is stable.

For a typical longitudinally stiffened cylinder, the asymmetric buckling load may be considerably below that of the axisymmetric case. The post-buckling behavior in this case appears to be similar to that of the isotropic cylinder[7].

For a typical circumferentially stiffened cylinder, only the axisymmetric load is possible since the asymmetric case generally leads to imaginary values of β. Thus, as the end shortening is increased beyond buckling, it follows the stable, horizontal axisymmetric path. However, at some point in this finite deflection region it is entirely possible that the β values associated with the asymmetric mode may become real resulting in the second bifurcation shown in Fig. 7. Beyond this point, the asymmetric path may be unstable.

The preceding discussion considered perfect cylinders and it is now instructive to consider the behavior of cylinders containing small initial imperfections. A possible loading path for such cylinders is shown by the dashed line in Fig. 7. As the load is increased, the

dashed line intersects the unstable asymmetric post-buckling curves for the longitudinally stiffened and isotropic cylinders considerably below the linear buckling load. It appears to be reasonable to assume that after the intersection point the asymmetric finite deflection paths would be followed. Thus, failure can occur considerably below the linear buckling load in the presence of small initial imperfections.

In the case of the circumferentially stiffened cylinder, the small stable axisymmetric post-buckling region plays a most essential role in significantly reducing the deleterious effects of initial imperfections. As illustrated in Fig. 7, the initial imperfection load path intersects the asymmetric finite deflection path well beyond the end shortening associated with buckling. Thus, failure occurs at a load not significantly below the axisymmetric buckling load depending upon the extent of the stable axisymmetric post-buckling region.

It is important to note that in all three cases failure generally occurs at the intersection of the initial imperfection path with the asymmetric finite deflections path. Thus, it is to be expected that the well known diamond buckle pattern should be observed at the conclusion of many cylinder experiments as shown in Fig. 8a. Under proper conditions, however, it should be possible to observe the formation of an axisymmetric buckle pattern for a circumferentially stiffened cylinder prior to failure in the diamond mode. In other cases such as an orthotropic elastic cylinder circumferentially stiffened (high α), the axisymmetric mode was actually observed[4] at the conclusion of the test as shown in Fig. 8b.

Plastic Cylinders

A schematic representation, based in part on Lee's analysis[5,9] of the post-buckling behavior of plastic isotropic moderate length cylinders, is illustrated in Fig. 9 in terms of the axisymmetric buckling parameters. The two cases shown are for the proportional limit region where the two buckling modes are slightly different and the yield region where the two buckling modes are significantly different.

Considering the yield region first, it can be observed that the stable axisymmetric post-buckling region is relatively large in extent by virtue of the significant separation of the asymmetric and axisymmetric buckling loads. As a consequence, cylinders containing small initial imperfections and following the dashed line in Fig. 9b tend to fail upon reaching the axisymmetric load. Here, failure occurs without intersection of the initial imperfection and unstable post-buckling asymmetric paths.

Thus, it can be anticipated that the axisymmetric buckle mode

should be observed at the conclusion of the test and that the failure load should be in good agreement with the axisymmetric buckling load. This is indeed the case for the test data shown in Fig. 6. Initial imperfections can be expected to play a negligible role in this case[9].

The probable conditions in the proportional limit region are depicted in Fig. 9a. Here, the stable axisymmetric post-buckling region is sharply reduced as compared to Fig. 9b by virtue of the small separation of the two buckling loads. As a result, the initial imperfection load path can intersect the unstable asymmetric post-buckling path and thus fail well below the axisymmetric and asymmetric buckling loads. Such cylinders would fail in the diamond buckle pattern and initial imperfections are significant here[9]. It is believed that such behavior is associated with the 7075-T6 test points in Fig. 6 that exhibited asymmetric buckles at failure.

CONCLUDING REMARKS

The experimental and theoretical results reported herein present some very significant practical implications for the shell structures of launch and space vehicles. Use of orthotropic circumferential stiffening of shells through either ring stiffeners or possibly through circumferentially oriented filaments appears to be an attractive way to achieve an important improvement in structural reliability over that associated with isotropic cylinders. Improved structural reliability can be realized through the ability to predict the failing load with far greater accuracy than for the isotropic case and through the statistical aspects associated with the much smaller scatter of the circumferentially stiffened cylinder experiments.

REFERENCES

1. Becker, H. and Gerard, G., "Elastic Stability of Orthotropic Shells," Journal of the Aerospace Sciences, Vol. 29, No. 5, pp. 505-512,520, May 1962.

2. Gerard, G., "Plastic Stability Theory of Geometrically Orthotropic Plates and Cylindrical Shells," New York University Tech. Rep. SM 61-11, July 1961. (Journal of the Aerospace Sciences, accepted for publication).

3. Gerard, G., "Compressive Stability of Orthotropic Cylinders," New York University Tech. Rep. SM 62-4, May 1962.

4. Becker, H., Gerard, G. and Winter, R. W., "Experiments on Axially Compressive General Instability of Monolithic Circumferentially Stiffened Circular Cylindrical Shells," New York University Tech. Rep. SM 62-5, May 1962.

5. Lee, L. H. N., "Inelastic Buckling of Initially Imperfect Cylindrical Shells Subject to Axial Compression," Journal of the Aerospace Sciences, Vol. 29, No. 1, pp. 87-95, Jan. 1962.

6. Osgood, W. R., "The Crinkling Strength and the Bending Strength of Round Aircraft Tubing," NACA Rep. 632, 1938.

7. Moore, R. L. and Clark, J. W., "Torsion, Compression and Bending Tests of Tubular Sections Machined from 75S-T6 Rolled Round Rod," NACA RM 52125, Nov. 1952.

8. Thielemann, W. F., "New Developments in the Nonlinear Theories of the Buckling of Thin Cylindrical Shells," Aeronautics and Astronautics, Pergamon Press, 1960, pp. 76-119.

9. Gerard, G., "On the Role of Initial Imperfections in Plastic Buckling of Cylinders Under Axial Compression," Journal of the Aerospace Sciences, Vol. 29, No. 6, pp. 744-745, June 1962.

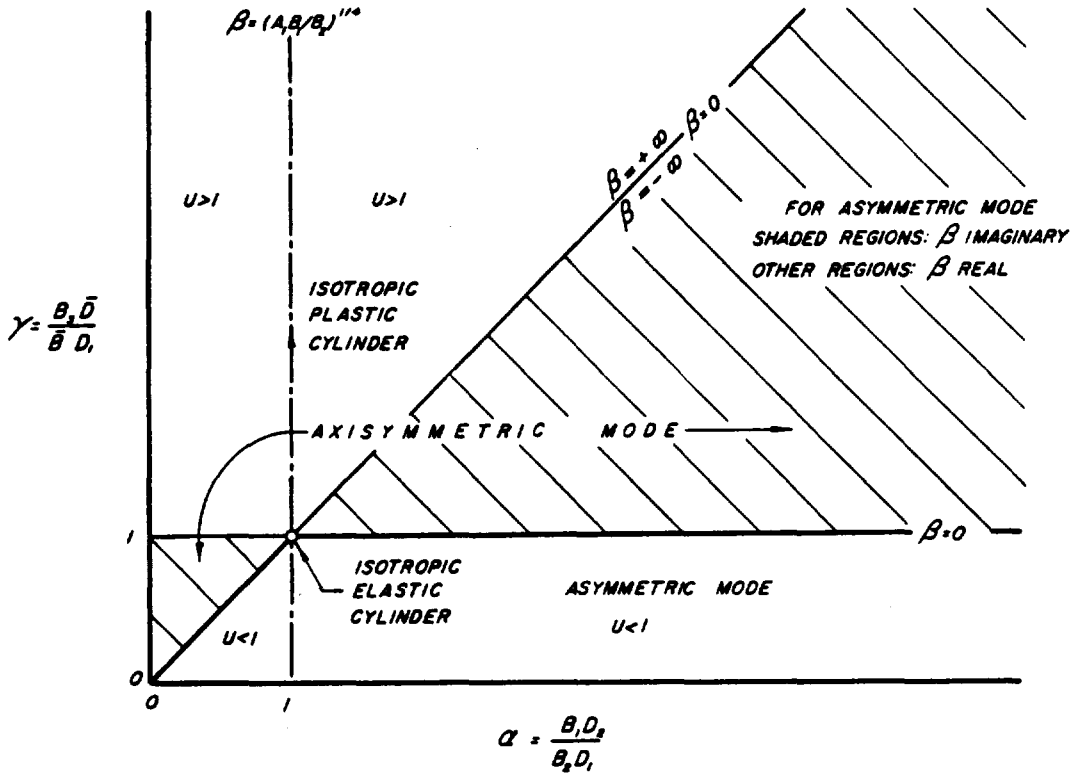

Figure 1.- Domains of β for the asymmetric mode.

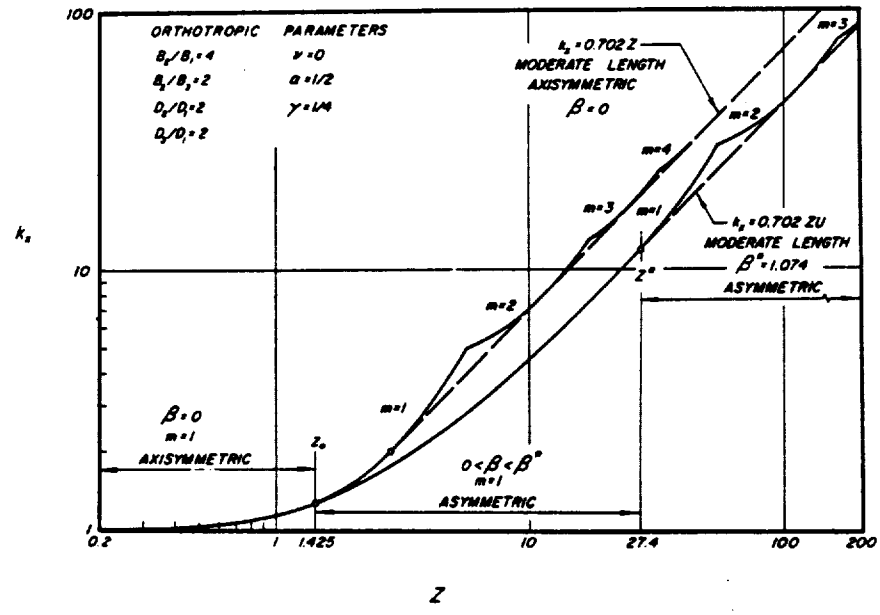

Figure 2.- Buckling coefficients for an elastic orthotropic cylinder. $B_2/B_1 = 4$, $B_2/B_3 = D_2/D_1 = D_3/D_1 = 2$ and $\nu = 0$.

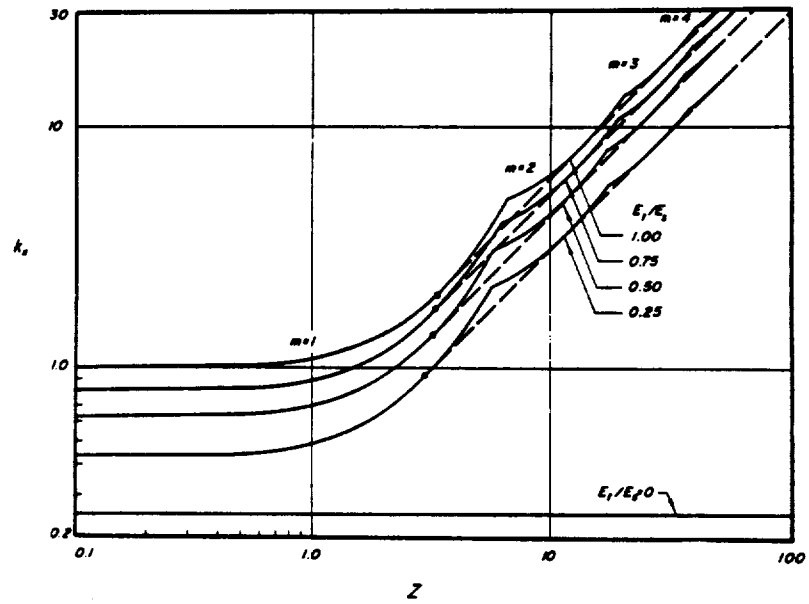

Figure 3.- Axisymmetric plastic buckling coefficients for isotropic cylinders.

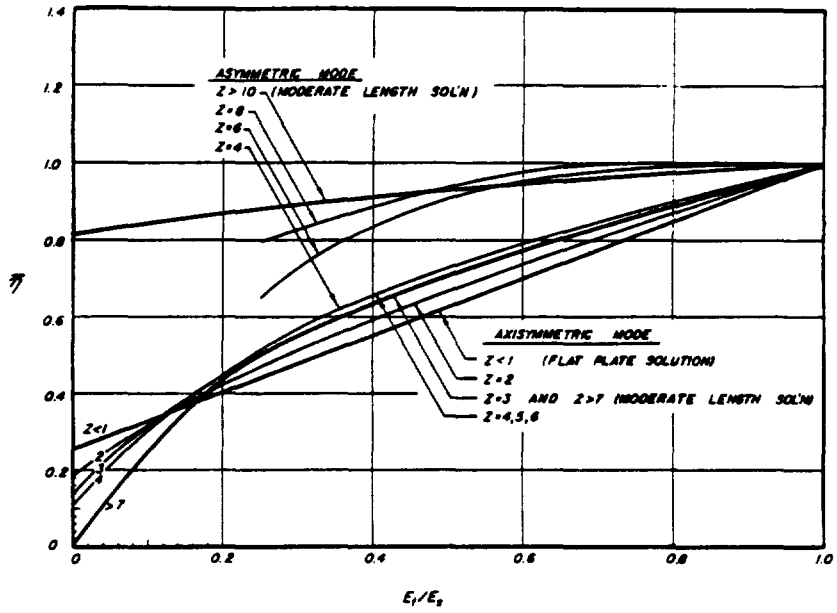

Figure 4.- Plasticity reduction factors as a function of E_t/E_s.

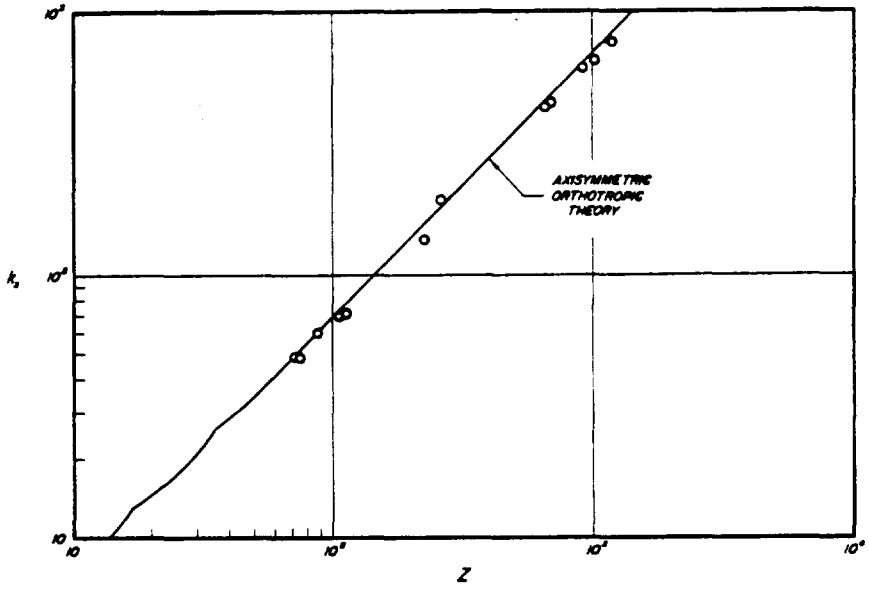

Figure 5.- Test data on elastic general instability of circumferentially stiffened cylinders in axial compression.

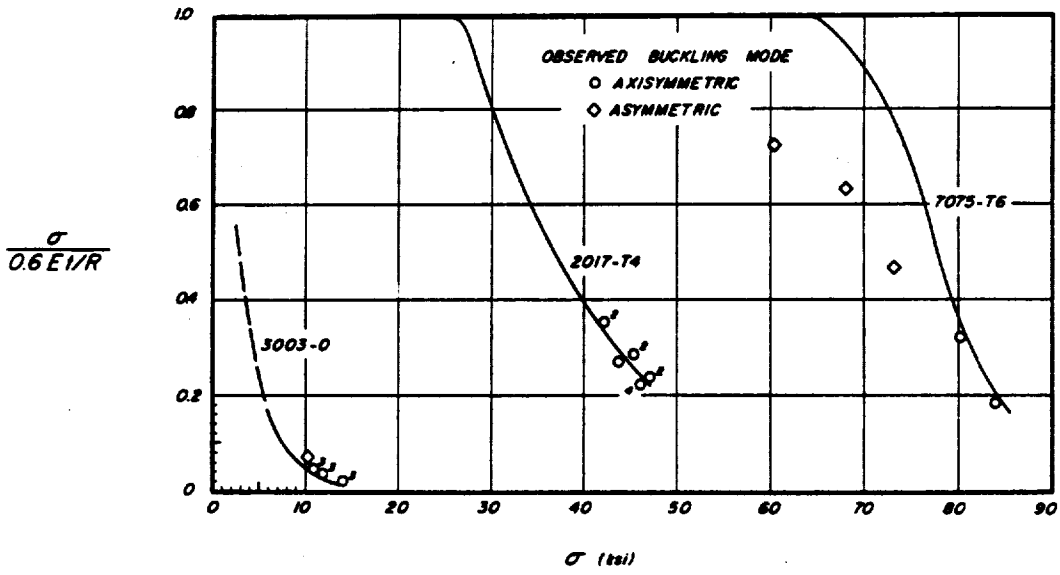

Figure 6.- Test data on plastic buckling of aluminum alloy isotropic cylinders under axial compression compared with axisymmetric theory.

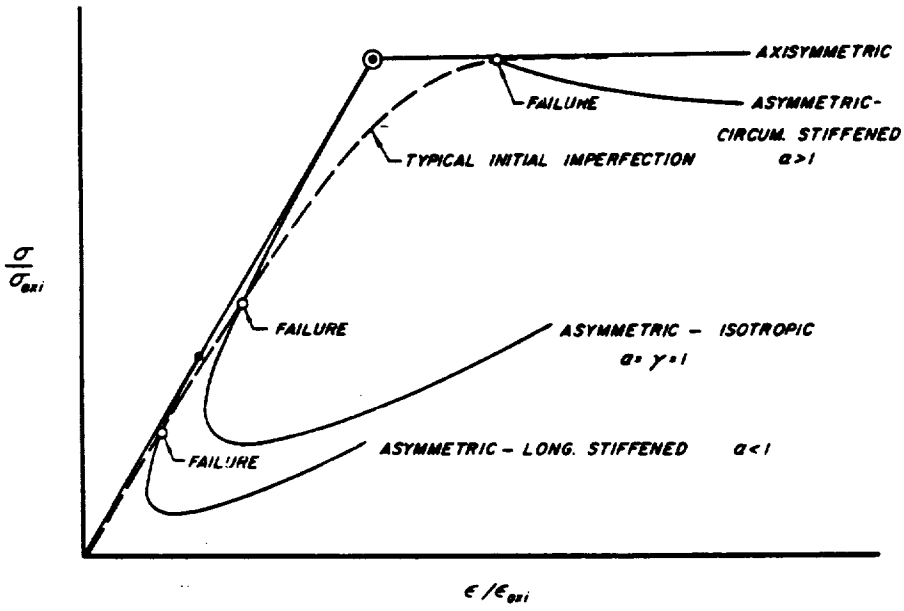

Figure 7.- Post-buckling behavior of moderate length, elastic, orthotropic cylinders (schematic).

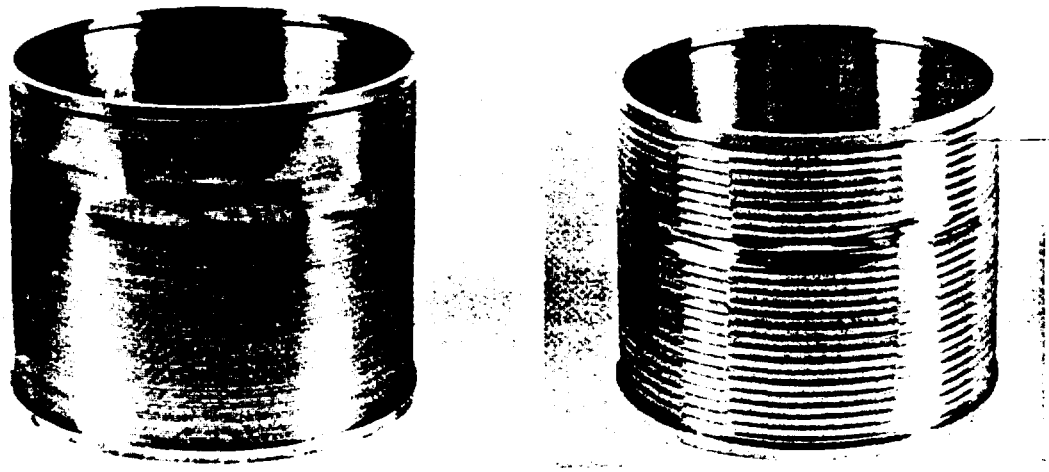

(a) $\alpha = 3.$ (b) $\alpha = 20.$

Figure 8.- Circumferentially stiffened buckle patterns at the conclusion of the test.

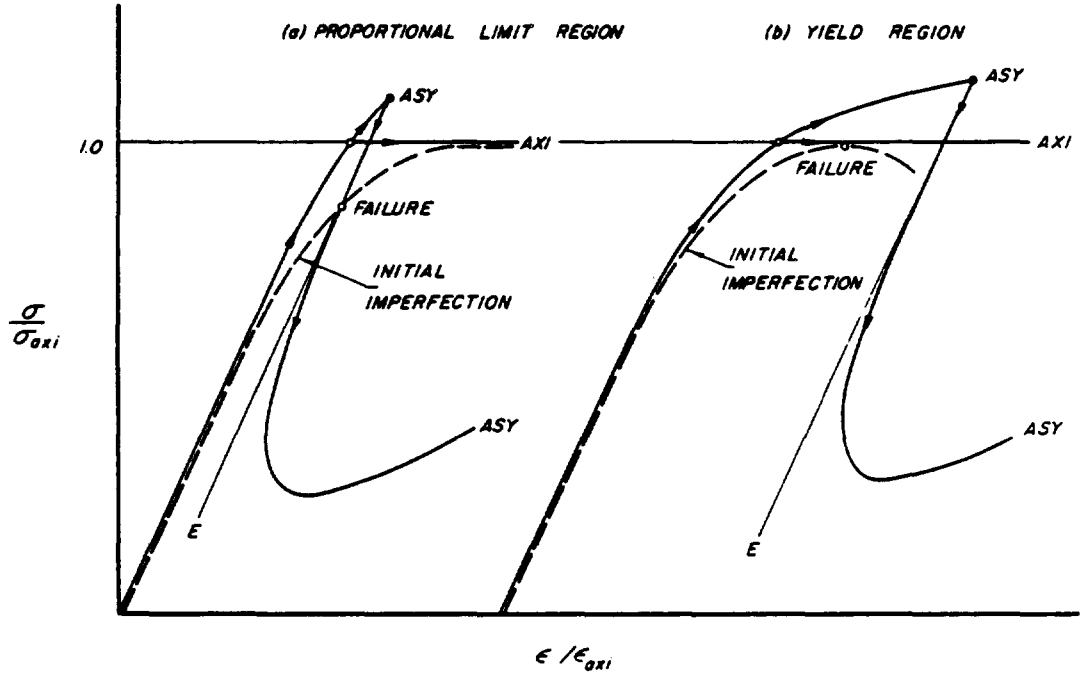

Figure 9.- Post-buckling behavior of moderate length, plastic, isotropic cylinders (schematic).